Bearing Damage Manifested by Extremely High Half-Speed Subharmonic Vibration on a Steam Turbine Generator

John Yu and Nicolas Peton

February 17, 2023

SIRM 2023 – 15th International Conference on Dynamics of Rotating Machines, Darmstadt, Germany, 22nd – 24th February 2023

Bearing Damage Manifested by Extremely High Half-Speed Subharmonic Vibration on a Steam Turbine Generator

John J. Yu [1], Nicolas Péton [2]
[1] Bently Nevada, Baker Hughes, Atlanta, USA, john.yu@bakerhuges.com
[2] Bently Nevada, Baker Hughes, Nantes, France, nicolas.peton@bakerhuges.com

Abstract

Parametric excitation can occur on a rotor-bearing system with subharmonic or fractional frequency vibration response if the stiffness has a sudden change over a fraction of its orbit. This can be explained from the Jeffcott rotor model, simplified into the standard Mathieu Equation. This paper focus on the exactly half-speed subharmonic vibration phenomenon. A corresponding real case of fluid film bearing damage is then presented on a steam turbine generator. Vibration reached over full scale of 508 microns (20 mil pp) at generator drive end bearing and therefore tripped the machine. The major vibration component that tripped the unit was exactly half-speed subharmonic frequency at a level of over 500 microns. The root-cause was found to be due to bearing damage. Why the half-speed subharmonic vibration occurred at such a high level that tripped the machine is fully explained in this paper. Other vibration plots including orbit, spectrum, and shaft centreline are also presented for vibration diagnostics. Rubs occurred but were not believed to be the root-cause of half-speed subharmonic vibration.

Keywords

Parametric excitation, Half-speed subharmonic vibration, Fractional frequency vibration, Vibration diagnostics, Shaft centreline, Orbit, Rub

Nomenclature

x = rotor lateral deflection in horizontal direction
y = rotor lateral deflection in vertical direction
M = rotor mass
D = damping of the rotor-bearing system
$K(\Omega t)$ = time-varying stiffness of the rotor-bearing system
K_0 = original stiffness
ΔK = increased or decreased stiffness during part of vibration cycle
α = range where ΔK occurs
k = any positive integer
m = unbalance mass
r = radius of unbalance mass
φ = phase lag of unbalance mass
Ω = rotor speed
t = time

τ = dimensionless time variable
a_n = Fourier coefficient of cosine term
b_n = Fourier coefficient of sine term
δ = coefficient in Mathieu Equation
ε = coefficient in Mathieu Equation (same sign as ΔK in this paper)
ω_n = original natural frequency of the rotor-bearing system

1 Introduction

Sub-synchronous vibration can sometimes be difficult in finding its root-cause. Amplitude of sub-synchronous vibration that occurs due to an instability issue can often go beyond the danger level to trip the machine.

Sub-synchronous vibration at a frequency of around one-half of the rotational speed or typically below is sometimes called half-frequency whirl [1] due to fluid-induced instability in bearings or seals. Muszynska [2] demonstrated whirl frequency of around but just below ½X through both analytical and experimental approaches. Many analytical and experimental results such as those by Crandall [3] and Childs [4] in addition to reference [1] do not support the notion of exact ½X whirl due to fluid-induced instability. It is believed that the exact ½X vibration is caused by parametric excitation due to non-linear or step-changing stiffness within the shaft orbit. Ehrich [5] published his observation of ½X vibration in an aircraft gas turbine engine and called it as subharmonic vibration to distinguish it from general sub-synchronous vibrations. Bently in [6] demonstrated his experimental results of this fractional frequency and named "normal-tight" and "normal-loose" conditions. Childs in [7] published some analytical work to explain Bently's work. Muszynska [8] presented partial rub experimental results with shaft orbit shape "8" containing the ½X component. Yu [9] presented three cases of ½X vibration.

This paper first demonstrates theoretically how subharmonic ½X is possible from a simple Jeffcott rotor model. Then a real case of ½X subharmonic vibration on a steam turbine generator is presented. Vibration plots including orbit, spectrum, and shaft centreline are illustrated for vibration diagnostics to help diagnose the malfunction.

2 Theory

The Jeffcott rotor model as shown in Figure 1 is employed to drive parametric excitation solution of ½X subharmonic vibration. Flexible bearing supports, represented by an asymmetric spring and dashpot array, are combined with a lumped mass. To simplify the solution, only one directional motion (in the horizontal direction) is described in terms of displacement *x*.

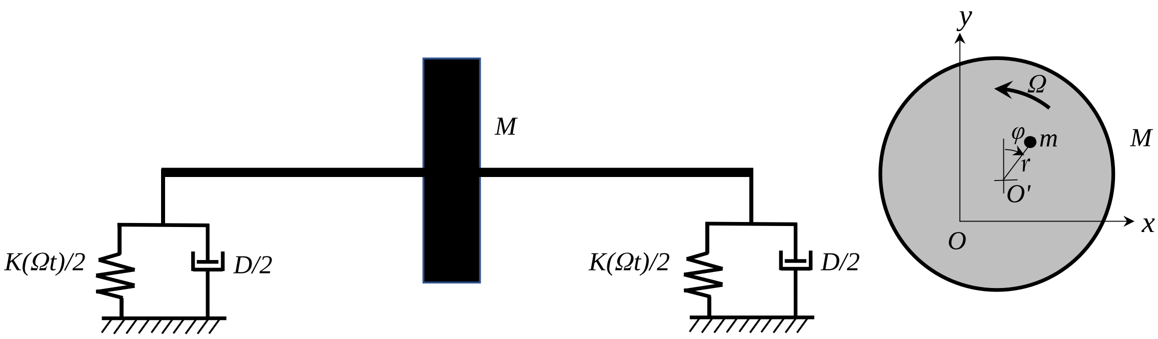

Figure 1: Jeffcort Rotor on flexible bearing supports

The rotor with lumped mass *M* and rigid shaft is supported by flexible bearings with stiffness *K(Ωt)* and damping *D*. Ω is the rotor speed, and *t* is time. The movement of the disk centre *O'* is described by displacement in horizontal and vertical displacements *x* and *y* in the fixed reference frame *Oxy*. Mass unbalance is expressed by *m* with radius *r* and phase lag φ relative to the top dead center.

Let us only consider the motion in the y-direction. The equation of motion of the Jeffcott rotor model in the y-direction as shown in Figure 1 can be given by

$$M\frac{d^2y}{dt^2}+D\frac{dy}{dt}+K(\Omega t)y=mr\Omega^2\cos(\Omega t-\varphi) \tag{1}$$

In some circumstance, stiffness changes within each vibration cycle. It could be decreased (normal-loose) or increased (normal-tight) for part of synchronous 1X vibration cycle. To reflect this change of stiffness, as shown in Figure 2, $K(\Omega t)$ can be modelled by the following periodic step-function:

$$K(\Omega t)=\begin{cases}K_0, & \text{for } 2(k-1)\pi\le\Omega t<2k\pi-\alpha\\ K_0+\Delta K, & \text{for } 2k\pi-\alpha\le\Omega t\le 2k\pi\end{cases} \tag{2}$$

where K_0 is original stiffness, ΔK is the change of stiffness, α is the range corresponding to the change of ΔK, and k can be any positive integer. Equation (2) can be expressed as Fourier series in the following:

$$K(\Omega t)=\frac{a_0}{2}+\sum_{n=1}^{\infty}\left(a_n\cos n\Omega t+b_n\sin n\Omega t\right) \tag{3}$$

where

$$a_n=\frac{1}{\pi}\int_0^{2\pi}K(\Omega t)\cos n\Omega t\; d(\Omega t)$$

$$b_n=\frac{1}{\pi}\int_0^{2\pi}K(\Omega t)\sin n\Omega t\; d(\Omega t)$$

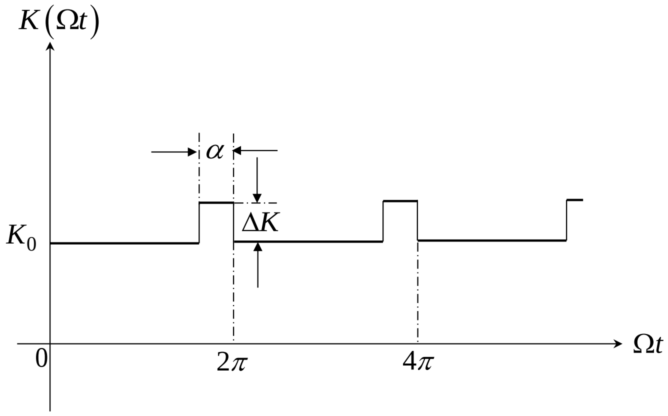

Figure 2: Time-dependent stiffness varying within each synchronous 1X vibration cycle

Thus time-dependent stiffness $K(\Omega t)$ can be given by

$$K(\Omega t)=K_0+\frac{\alpha\Delta K}{2\pi}+\frac{2\Delta K}{\pi}\sum_{n=1}^{\infty}\frac{\sin\frac{n\alpha}{2}}{n}\cos\left(n\Omega t+\frac{n\alpha}{2}\right) \tag{4}$$

A dimensionless time variable τ is introduced as follows:

$$\tau=\frac{1}{2}\Omega t+\frac{1}{4}\alpha \tag{5}$$

Since the homogenous solution of Eq. (A1) is of interest only to examine instability issues, the unbalance force term is neglected. To examine possible ½X parametric excitation due to time-dependent stiffness, case $n=1$ in Equation (4) is considered. Inserting Equation (4) with $n=1$ and Equation (5) into Equation (1) yields

$$\frac{d^2x}{d\tau^2}+\frac{2D}{M\Omega}\frac{dx}{d\tau}+\left(\delta+2\varepsilon\cos 2\tau\right)x=0 \tag{6}$$

where

$$\delta=\frac{1}{\left(\frac{1}{2}\Omega\right)^2}\frac{K_0+\frac{\alpha\Delta K}{2\pi}}{M} \tag{7}$$

$$\varepsilon=\frac{1}{\left(\frac{1}{2}\Omega\right)^2}\frac{\Delta K\sin\frac{\alpha}{2}}{\pi M} \tag{8}$$

To obtain approximate solution of instability region and frequency, the damping term in Equation (6) is neglected. Thus, Eq. (A6) is simplified into the standard Mathieu Equation [10] as follows:

$$\frac{d^2x}{d\tau^2}+\left(\delta+2\varepsilon\cos 2\tau\right)x=0 \tag{9}$$

The principal instability region is approximately determined by

$$\left|\delta-1\right|<\left|\varepsilon\right| \tag{10}$$

and the unstable solution is dominantly composed of $\cos\tau$ and $\sin\tau$ terms. As indicated in Equation (5), this is exactly the ½X vibration.

Assume that α is small. Thus $\sin\frac{\alpha}{2}\approx\frac{\alpha}{2}$. From Equation (10), unstable speed region due to step-changing stiffness is determined by

$$2\omega_n<\Omega<2\omega_n\sqrt{1+\frac{\alpha\Delta K}{\pi K_0}},\quad \text{for } \Delta K>0 \tag{11}$$

and

$$2\omega_n\sqrt{1+\frac{\alpha\Delta K}{\pi K_0}}<\Omega<2\omega_n,\quad \text{for } \Delta K<0 \tag{12}$$

where

$$\omega_n=\sqrt{\frac{K_0}{M}}$$

is obviously the original natural frequency of the rotor-bearing system. Equations (11) and (12) can be regarded as normal-tight and normal loose cases, respectively.

3 Real Case

This is a cross-compound steam turbine generator unit with HP turbine (3600 rpm) and LP turbine (1800 rpm), as shown in Figure 3. Its rated power output is 775 MW. High vibration excursion occurred on the generator of the HP section. It consists of HP and IP rotors along with the hydrogen-cooled generator.

Figure 3: cross-compound steam turbine generator

The radial vibration probes are mounted at 45° left (Y-probe) and 45° right (X-probe) relative to the top dead center (TDC). There is also a dual-probe setup at each bearing at 30 degrees right, which takes both shaft relative and seismic data to generate shaft absolute readings. They are numbered in order from turbine to generator. The Keyphasor® probe is located at about 90 degrees right relative to the TDC when looking from the turbine to the generator.

After a scheduled outage, startup vibration data was monitored and obtained by using Bently Nevada ADRE® Sxp software and 408 DSPi Data Acquisition System.

3.1 ½X vibration excursion

When the HP generator was brought up to a constant warmup speed of 1800 rpm (half speed of rated 3600 rpm), vibration reached over 508 μm pp (20 mil pp) at the generator drive end bearing (Brg#5 as shown in Figure 4) and therefore tripped the unit.

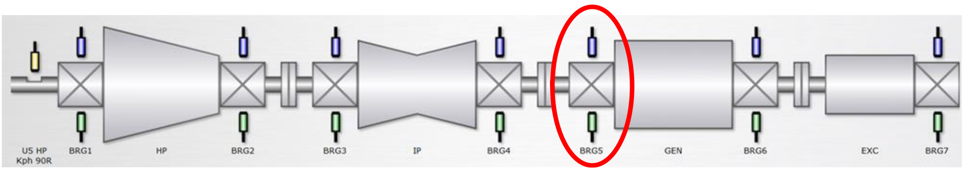

Figure 4: HP generator machine train diagram

Figure 5 is a vibration trend plot containing direct (broad-band frequency), 1X, ½X, and 2X components measured from Brg#5 X-probe. During initial 5 minutes at 1800 rpm, vibration was very low and stable. Then the 1X synchronous vibration started to change with amplitude being up and down. After 2 hours and 20 minutes, the ½X suddenly appeared with amplitude up to 518 μm pp, causing the unit to trip.

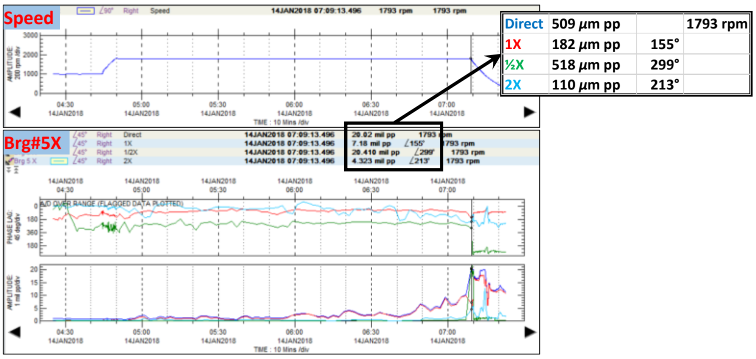

Figure 5: Direct, 1X, ½X, and 2X vibration trend plot at 1800 rpm with ½X up to 518 μm pp

Figure 6 shows orbit plots at 1800 rpm from low to high vibration amplitude in red color. The first 5 orbits were mainly due to the 1X vibration. Then the ½ X vibration occurred and tripped the unit. The last orbit in green color was at 1780 rpm during shutdown after the trip. Since the full scale was set at 508 um pp (20 mil pp) in ADRE configuration, amplitude over that level was truncated. It had not been expected that vibration amplitude would exceed this level.

Figure 6: Orbit plots at Brg#5 during vibration excursion at 1800 rpm followed by trip at 1780 rpm

Figure 7 shows full-spectrum waterfall plot during the run. When the 1X vibration was dominating, vibration amplitude was low. Then the abnormal ½ X vibration occurred, accompanied by its multiples 1X, $\frac{3}{2}$ X, 2X, etc**.**

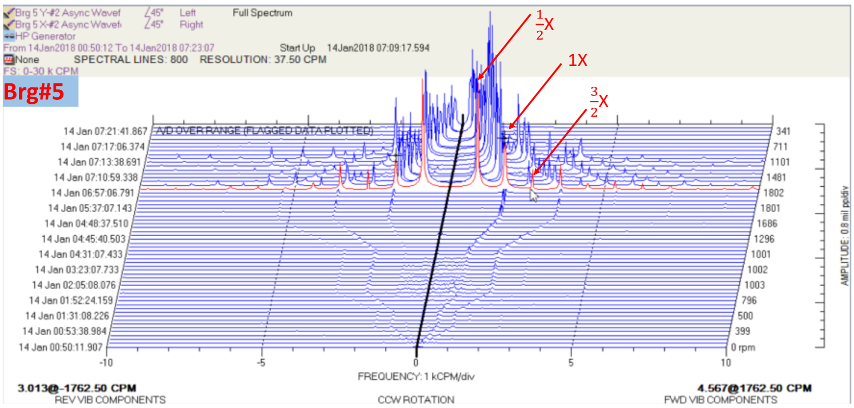

Figure 7: Waterfall plot at Brg#5 during the run

3.2 Diagnostics of the ½X vibration excursion

The root-cause of the abnormal ½ X vibration needed to be found out before the unit could safely start again. Whether it was exactly ½ X or close to ½ X would make a big difference in malfunction diagnostics. Figure 8 shows the orbit/timebase plot at Brg#5 at 1780 rpm. Though X directional amplitude was beyond the 508 μm pp (20 mil pp) full scale, Keyphasor dots were available on the plot plus Y directional amplitude was not affected. These Keyphasor dots were clearly locked at the same location in the orbit and timebase. Therefore, the sub-synchronous vibration was exactly ½ X subharmonics, not close to 0.5X.

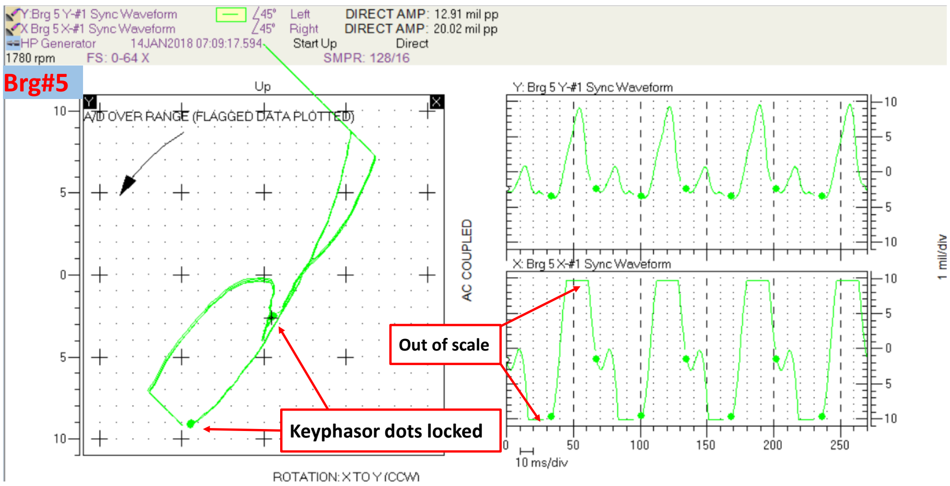

Figure 8 Evidence of exactly ½ X subharmonics from Keyphasor dots

As to whether it was a normal-tight or normal loose case as shown in Equation (11) or (12), the natural frequency of the generator rotor-bearing system would need to be examined. Figure 9 presents Bode plots measured by 4 proximity probes on the generator DE and NDE bearings. The first critical speed was 991 rpm as shown in Figure 9, which can be interpreted as the natural frequency of the generator rotor-bearing system ω_n .

The ½X subharmonics occurred at 1631 to 1800 rpm during shutdown. Therefore, this situation fits the normal-loose condition described in Equation (11), i.e.,

$$2\times 991\sqrt{1-\frac{\alpha|\Delta K|}{\pi K_0}} < \Omega < 2\times 991 \text{ rpm}$$

where $\Delta K < 0,$ and $\Omega = 1631-1800$ rpm . The value of the left term is obviously around 1631 rpm. Certainly there is no need to evaluate the exact values of α and ΔK.

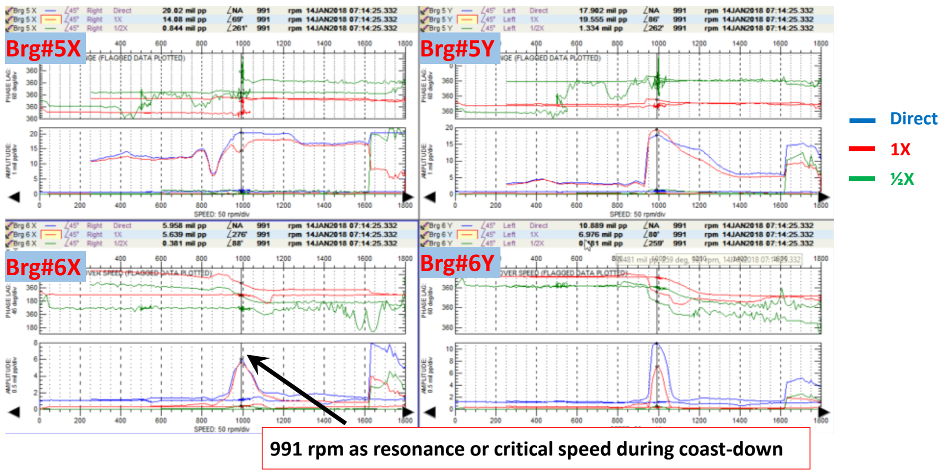

Figure 9: Bode plots measured by 4 proximity probes at generator bearings during coastdown

As to the root- cause of the normal-loose condition, shaft centerline plots were examined to see journal positions relative to the bearing walls. It was surprised to observe that shaft centerline position at Brg#5 moved well beyond its bearing clearance wall, based on the startup reference point taken during the startup. During the outage, the as-left bearing diametral clearance in the vertical direction was measured as 0.610 mm (24 mils). However, the current position appeared that the bearing clearance had significantly increased by approximately 1 mm (40 mils). Therefore, bearing damage was strongly suspected. Normally bearing wipe-up can be easily detected via bearing metal temperature spiking. At that time, unfortunately bearing metal temperature reading was invalid, and therefore only vibration data could be used to diagnose any possible malfunctions.

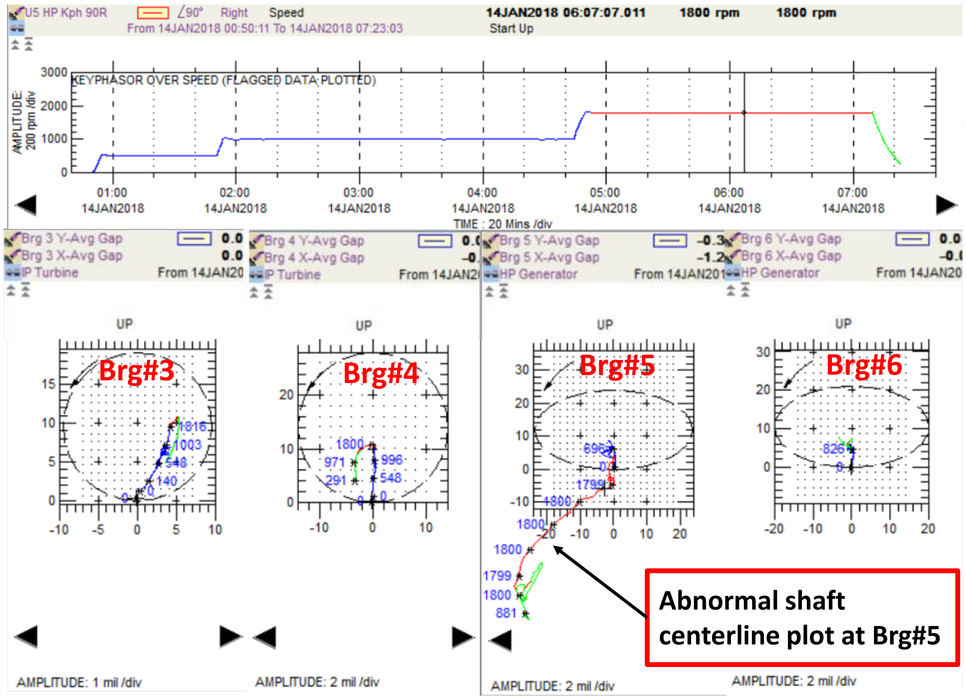

Figure 10: Shaft centerline plots from Brg#3 to Brg#6

One thing regarding changing 1X vibration prior to the onset of ½ X subharmonic vibration remained unexplainable in the very beginning. Later further in-depth data review pinpointed a possibility of rub events. Figure 11 shows 1X trend and polar plots measured by Brg#5 X probe. The 1X vector increased against shaft rotation, behaving as the Newkirk effect. The other evidence of rub was the high 1X amplitude of over 254 μm pp (10 mil pp) measured by Brg#5 X probe from 750 rpm to 250 rpm during shutdown, as shown in Figure 9, indicative of strong shaft bow resulted from rubs.

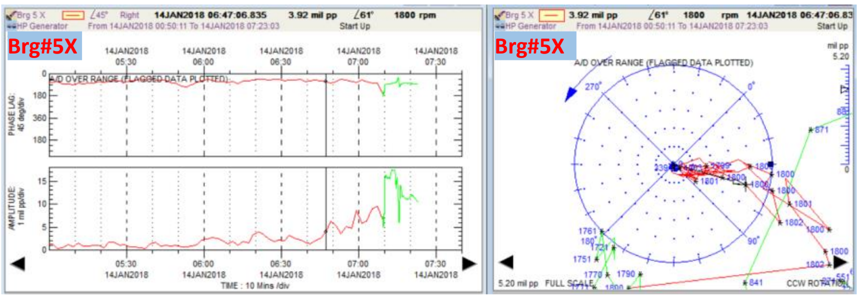

Figure 11: 1X vibration excursions prior to the onset of ½ X subharmonic measured by Brg#5 X probe

3.3 Inspection and findings

An inspection was requested to open the machine near Brg#5 area. The bearing was found to be indeed wiped at the left bottom, as shown in Figure 12, with additional 1.067 mm (42 mils) clearance due to wear beyond as-left clearance of 0.610 mm (24 mils) in the vertical direction, matching the diagnosis. Obviously, the wear was due to the journal rubbing against the babbitt surface.

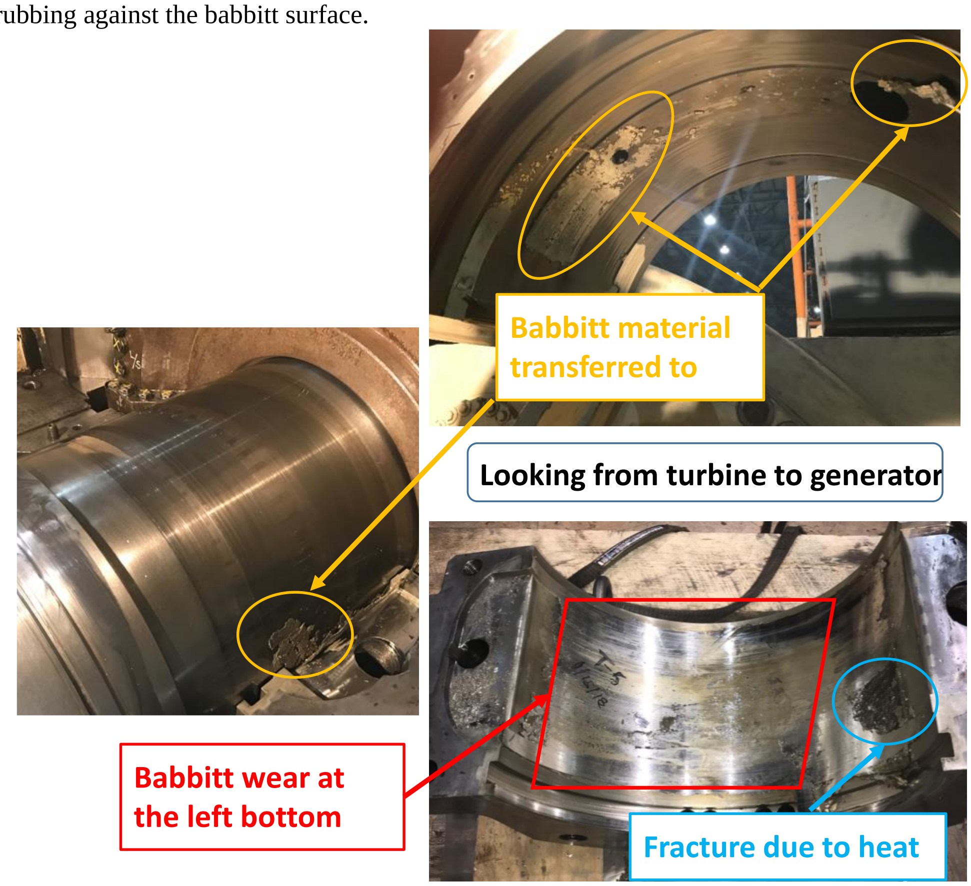

Figure 12: Bearing damages found during an inspection

It was found that a fine strainer was mistakenly left in place, causing oil reduction and starvation, and finally wiping up the bearing. This was believed to be the root-cause. The bearing was shipped offsite to be re-spun.

It appeared that rubs had occurred on inner and outer oil deflectors at Brg #5 as well as that at the adjacent Brg #4 generator side. All these three oil deflectors were shipped offsite for teeth replacement.

It also seemed that Brg#5 hydrogen seal casing oil deflector had been rubbed, which was then replaced with new one.

The clearance and alignment condition were found to be acceptable at the adjacent Brg #4 turbine side oil deflector.

3.4 Resolution and final vibration results

The bearing was repaired by refurbishing its babbitt and re-installed correctly. Several damaged oil deflectors were replaced with new ones. The bearing lube oil system was ensured to function normally.

The unit was then restarted successfully with acceptable vibration level without any abnormal vibration behavior. Figure 13 shows a normal full-spectrum waterfall plot measured by Brg#5 X and Y probes. Note that a seemingly ½ X in a very low level was not due to its own HP rotor vibration. It was the 1X LP (1800 cpm at rated speed) vibration transmitted from the same foundation.

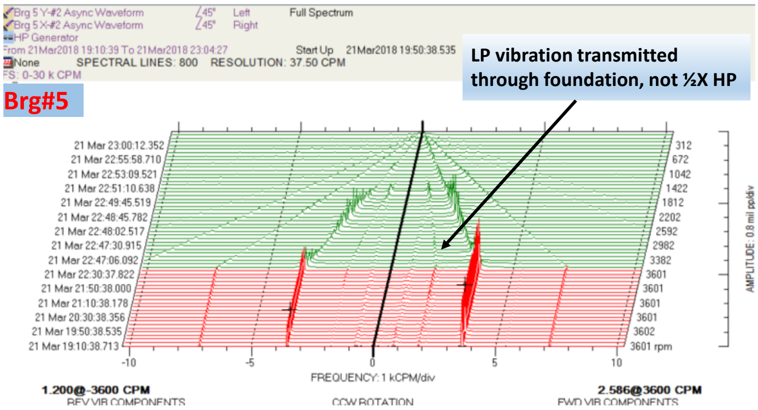

Figure 13: Normall full-spectrum waterfall plot at Brg#5

The corresponding shaft centerline plot also became normal. The journal position was moving within the normal range, as shown in Figure 14.

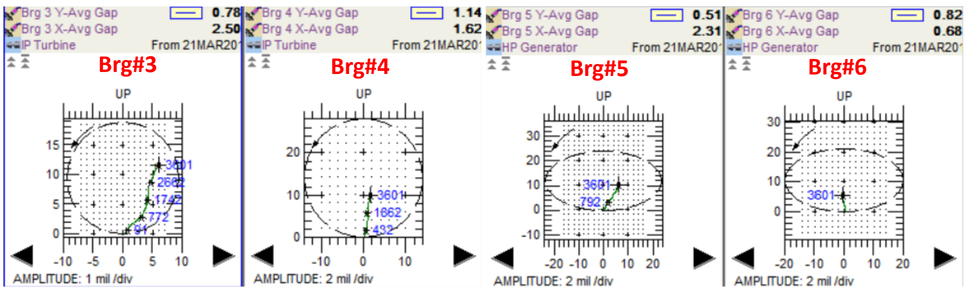

Figure 14: Normal shaft centerline plot at Brg#5 and adjacent bearings

4 Discussion and Conclusions

Parametric excitation analysis on why ½X vibration can occur is presented, which includes unstable speed region by using the Jeffcott rotor model. Step-changing nonlinear stiffness function is modelled and expanded into Fourier series. The homogeneous equation of the Jeffcott rotor model is then simplified into the well-known Mathieu Equation, which yields the solution of instability.

Two conditions are needed to make this unstable ½X vibration possible. First, stiffness would need a step-change within a cycle or orbit of synchronous 1X vibration. In the real case presented here, the bearing surface damage resulted in the large clearance within the fluid bearing. Thus, the bearing stiffness had a step-change likely at the top right of the orbit. In other words, on part of the orbit trajectory at the top right, oil film support could not be provided and bearing stiffness had a sudden decrease from K_0 to $K_0 + \Delta K$, where $\Delta K < 0$. Secondly, rotor speed would have to be approximately at twice the natural frequency of the rotor-bearing system. For the current case, when speed Ω is between 1631 to 1800 rpm, close but slightly lower than 2 times the natural frequency of 991 rpm.

Rubs occurred in this case, but it was manifested by 1X synchronous vibration excursion. In other words, it was not the root-cause of the ½X subharmonic vibration. Had the natural frequency been 815 rpm or below, the ½X subharmonic vibration would have been resulted from rubs as ΔK could be considered as positive due to rub contact leading to a step-increase in stiffness.

In addition to correct determination if sub-synchronous vibration is exactly ½ X subharmonics or close to 0.5X sub-synchronous vibration, review of shaft centerline plot is very important to help diagnose the root-cause of the vibration.

References

[1] Ehrich, F.F., 1999, Handbook of Rotordynamics, Krieger Publishing Company, Malabar, FL.

[2] Muszynska, A., 1986, "Whirl and Whip – Rotor/Bearing Stability Problems," J. Sound Vib., 110, pp.443-462.

[3] Crandall, S., 1990, "From Whirl to Whip in Rotordynamics," IFToMM 3rd Int. Conf. on Rotordynamics, Lyon, France, pp. 19-26.

[4] Childs, C., 1993, Turbomachinery Rotordynamics: Phenomena, Modeling, and Analysis, John Wiley & Sons, New York.

[5] Ehrich, F.F., 1966, "Subharmonic Vibration of Rotors in Bearing Clearance," ASME Paper No. 66-MD-1.

[6] Bently, D.E., 1974, "Forced Subrotative Speed Dynamic Action of Rotating Machinery," ASME Paper No. 74-Pet-16.

[7] Childs, C., 1982, "Fractional Frequency Rotor Motion Due to Non-Symmetric Clearance Effects," ASME J. Eng. Power, pp. 533-541.

[8] Muszynska, A., 1984, "Partial Lateral Rotor to Stator Rubs," Proceedings of the 3rd Int. Conf., Vibration in Rotating Machinery, IMechE, C281/84, York, UK, pp227-236.

[9] Yu, J. J., 2010, "Onset of 1/2X Vibration and Its Prevention", Transactions of the American Society of Mechanical Engineers, Journal of Engineering for Gas Turbines and Power, Vol. 132, 022502.

[10] Meirovitch, L. 1975, Elements of Vibration Analysis, McGraw-Hill, New York.